www.MaterialsViews.com

ADVANCED FUNCTIONAL MATERIALS
www.afm-journal.de

FULL PAPER

Energy Transfer in Nanotube-Perylene Complexes

Friederike Ernst, Timm Heek, Antonio Setaro, Rainer Haag, and Stephanie Reich*

A functional surfactant designed to solubilize and individualize nanotubes efficiently in aqueous media and to form energy transfer complexes with the carbon nanotubes through π–π stacking is presented. Upon excitation of the adsorbed perylene unit an emission from the nanotubes is observed that indicates a successful excitation transfer. The efficiency of the indirect excitation via the adsorbant is of the same order of magnitude as the direct excitation of the nanotubes. Under optimized preparation conditions the pH independent perylene-imido-diester compound isolates and solubilizes carbon nanotubes in biocompatible aqueous environments without additional surfactants. The resulting solutions are stable over many months.

1. Introduction

Single walled carbon nanotubes (SWNTs) have unique electronic and optical properties making them equally attractive for fundamental research and potential applications.[1,2] Of special interest is their bright emission in the near and mid-infrared, which also covers the important window of tissue transparency.[3,4] Light emission and other one-dimensional signatures only manifest themselves in isolated tubes, i.e. in individual tubes and very small bundles. An efficient way of separating large quantities of tubes is dispersion in aqueous solution. Carbon nanotubes are, however, strongly hydrophobic and require a dispersing agent.[5] While classical surfactants display a non-specific hydrophobic interaction, π–π stacking is based on orbital overlap between surfactant and nanotube. The inclusion of aromatic moieties with ensuing π–π interaction has been demonstrated to have a positive effect on dispersion efficiencies of surfactants.[6]

Up to now, typical surfactants for nanotube dispersion have no additional functionalities. An intriguing idea is to combine the dispersion in aqueous solution with other features. A highly desirable functionality is a surfactant-nanotube complex in which excitation transfer takes place from the surfactant to the nanotube, see **Figure 1**, top panel. This allows exciting multiple types of nanotubes with one excitation energy, greatly facilitating applications such as bioimaging and biodetection,[7,8] as well as light harvesting in organic photovoltaic devices.[9] Excitation transfer in nanotube complexes has been previously reported in both covalently[10] and non-covalently functionalized tubes.[11–14] Covalent functionalization, however, results in lattice defects, compromising the unique optoelectronic properties, while the non-covalently functionalized tubes were mostly obtained through solubilization with Triton X-100, toluene and other organic solvents, which degrade the nanotube optical properties and have poor long-term stability. Secondly, the dependence on organic solvents precludes the utilization of the nanotube-adsorbant excitation transfer complexes in biocompatible environments. In micelle swelling this problem is circumvented at the cost of complicating the process through the use of two solvents, water and an organic solvent, and an additional surfactant. The organic solvent is subsequently removed, leaving behind sodium dodecyl sulfate (SDS) micelles with porphyrin-nanotube complexes in aqueous solution.[15] Moreover, energy transfer in water has been demonstrated at non-biological pH.[16] Another study reported an energy transfer between nanotubes and adsorbed perylenes; however, conclusive evidence of the transfer process, e.g., in photoluminescence, remained missing.[17]

We present a perylene-based surfactant comprising three sub-units. A perylene dye is combined with a polyglycerol dendron for water solubility and two alkyl chains for nanotube individualization. The surfactant forms a complex with the nanotubes in which excitation transfer takes place. The indirect excitation of the SWNTs through the surfactant has a quantum yield on the same order of magnitude as the direct excitation. Our complexes are highly stable in an aqueous solution with no apparent deterioration over the course of many months. As opposed to earlier perylene-compound surfactants[18] the terminations of our dendritic structure safeguard pH independence as required for utilization in biological environments.

2. Results and Discussion

2.1. Solubilization

A novel perylene-imido-diester, referred to as **C16**, was designed as a surfactant for the solubilisation of SWNTs. Its chemical structure is shown in the bottom panel of Figure 1. **C16** is composed

F. Ernst, Dr. A. Setaro, Prof. S. Reich
Freie Universität Berlin
Department of Physics
Arnimallee 14, 14195 Berlin, Germany
E-mail: f.ernst@fu-berlin.de

T. Heek, Prof. R. Haag
Freie Universität Berlin
Department of Chemistry
Fabeckstr 34/36, 14195 Berlin, Germany

DOI: 10.1002/adfm.201200784

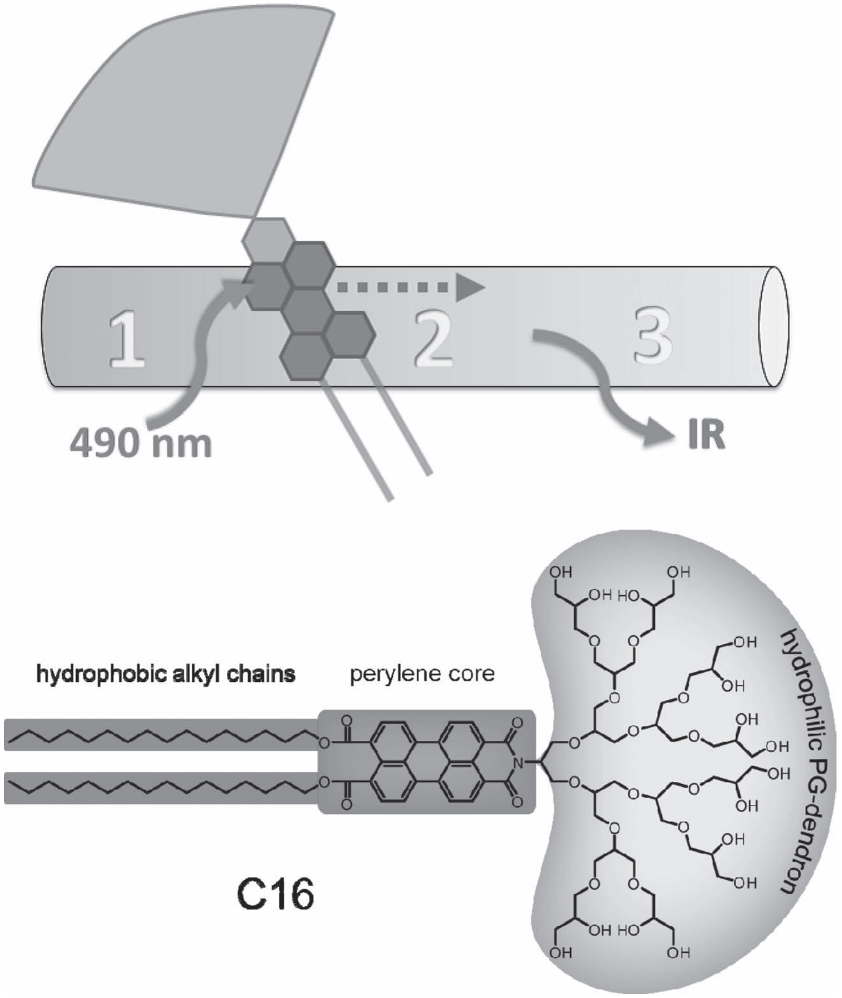

Figure 1. Top panel: Schematic depiction of the energy transfer process between perylene adsorbate and nanotube: upon excitation of the perylene surfactant **(1)** an excitation transfer takes place from the perylene into the nanotube **(2)**. Subsequently, a nanotube emission is seen in the IR **(3)**. The emission energy depends on the tube chirality. Bottom panel: Chemical structure of the investigated perylene-imido-diester (**C16**). **C16** possesses a perylene unit, a polygylcerol dendron and two alkyl chains composed of 16 carbon atoms each.

of three subunits that serve different functions. The aromatic core consists of a perylene derivative. Perylene derivative dyes have attracted a lot of attention in the nanotube community because they are planar, which facilitates π–π stacking.[16–24] Perylene-imido-diesters have an absorption of 420–550 nm and emission 520–700 nm. They are thus ideal candidates for the optical pumping of carbon nanotubes. The dye was combined with a polyglycerol dendron. Polyglycerol dendrons ensure water solubility[25] and are known to enhance biocompatibility of surfactants.[26] Finally, the hydrophobic alkyl chains proved indispensable for nanotube individualization. This rationally designed perylene-based surfactant was used to prepare stable nanotube suspensions, see Experimental Section. Photoluminescence excitation (PLE) measurements were conducted to probe the surfactant's ability to individualize SWNTs. The PLE signal strength is a good indicator of the quantity of individualized or near-individualized SWNTs of a given chirality.[27–30] **C16** is effective at individualizing and solubilizing nanotubes with a similar efficiency as SDS. A similar compound with no alkyl chains was unable to separate the tubes and hence did not yield a PLE signal. We conclude that the alkyl chains are imperative for debundling.

The ratio of **C16** to SWNTs was found to be of crucial importance for effective individualization and solubilization. Typical absorption features seen for SWNTs are the S_{11} transitions between 950 nm and 1350 nm and S_{22} transitions between 620 nm and 830 nm,[1] while the perylene compound has a broad absorption between 420 nm and 550 nm.[31]

Figure 2a shows the absorption spectra for different preparation concentrations of SWNTs (for a detailed protocol of the preparation procedure see Experimental Section) at a constant preparation concentration of **C16**. A gradual decrease of the signal from the free perylene is observed for nanotube preparation concentrations between 0.01 g/L and 0.13 g/L. The adsorbed **C16** shows up as a residual plateau in the perylene absorption region. Beyond this limit of 0.13 g/L, the sample looks clear and does not exhibit absorption features; the SWNTs and **C16** precipitated completely during centrifugation, leaving behind water.

Figure 2b represents the fraction of solubilized nanotubes and free **C16** as a function of CNT concentration. The squares give the difference in absorption between 481 nm, the maximum of the perylene absorption, and 402 nm, the baseline, and are thus a measure of the quantity of free **C16**. The reddish coloration of the solutions decreases with increasing nanotube preparation concentration. This is also seen in the photograph of the solutions (Figure S1, Supporting Information). The abundance of individualized nanotubes is estimated from the height of the characteristic SWNT features visible in the absorption spectrum from 600 nm upwards. The intensity of the absorption band at 740 nm was used as an indicator of the quantity of nanotubes, plotted as circles in Figure 2b. This quantity rises with the SWNT preparation concentration up to 0.13 g/L and then drops to zero at 0.15 g/L. Panel **c** shows the relative peak intensities of the two perylene transitions, 0 → 1 at 481 nm and 0 → 0 at 520 nm, corresponding to the self-aggregated and nanotube-adsorbed forms, respectively.[18,32,33] At low nanotube preparation concentrations the free **C16** forms micelles, resulting in a large 0 → 1 peak. With increasing tube concentration, the 0 → 0 transition becomes more prominent, indicating monomeric adsorption onto tubes.[18]

Based on the data in Figure 2, we suggest that nanotube solubilization through **C16** can be described in terms of three regimes in dependence of the initial SWNT concentration: 1) At low SWNT starting concentrations there is plenty of free **C16**, lending the solution a reddish color; the tubes get individualized

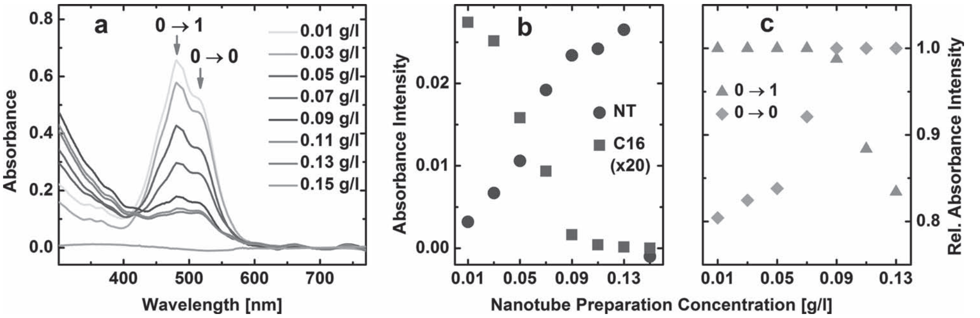

Figure 2. a) Absorbance measurements of **C16** samples prepared with different concentrations of nanotubes. b) The difference in absorbance between 744 nm and 706 nm (circles) quantifies the magnitude of the characteristic undulating SWNT features upwards of 600 nm and is thus a measure for the abundance of SWNTs in the solution. The difference in absorbance between 481 nm and 402 nm (squares) gives the height of the 481 nm perylene peak and hence the quantity of free **C16** molecules in the solution. The **C16** absorption is scaled down by a factor of 20. c) The relative intensities of the peaks of the two perylene transitions, 0 → 1 at 481 nm (triangles) and 0 → 0 at 520 nm (diamonds), corresponding to the self-aggregated and nanotube-adsorbed forms, respectively.[18,32,33]

efficiently. The nanotube fluorescence signal is masked however by the free surfactant. Perylene-imido-diesters have a very high fluorescence quantum efficiency of ca. 95%[34] as compared to 3% for single suspended nanotubes,[35] or 0.05% for typical nanotube solutions[36] and thus mask the SWNT signal. 2) With increasing SWNT preparation concentration, a larger fraction of the **C16** molecules is adsorbed onto the now more plentiful tubes, leaving smaller quantities of free **C16** and larger quantities of individualized nanotubes, making the solution increasingly greyish and decreasingly reddish. At the optimal surfactant to tube ratio the fluorescence emission of the free **C16** is three orders of magnitude smaller compared to the lower SWNT concentrations (cf. Figure 4a). This justifies the assumption that the dynamic equilibrium which is reached at the working temperature is strongly skewed towards the adsorbed **C16**. The optimal starting concentration of SWNTs at a fixed molarity of C16 of 6×10^5 M was determined to be 0.11 g/L. 3) At even larger preparation concentrations of nanotubes **C16** is no longer able to individualize the tubes, adsorbing to bundles instead, and is accordingly centrifuged out, leaving an aqueous solution behind. This behavior can be seen in the 0.15 g/L track in Figure 2a.

The optimal nanotube-surfactant ratio was found to change with **C16** molarity; while counterintuitive at first, this can be understood in terms of the dynamic equilibrium between free and adsorbed **C16** molecules as we will discuss in detail elsewhere.

Studies on the SWNT solubilization capabilities of other perylene compounds (perylene-bisimide derivatives) were conducted previously.[23,24] However, the PLE signal intensity was found to be greatly reduced with respect to sodium dodecyl benzene sulfonate (SDBS) dispersed SWNTs. The authors attributed this to the homogeneity of the surfactant coverage and backed this up with subsequent recovery of photoluminescence through addition of SDBS.[23] We suggest that the SWNT and perylene-compound concentrations used[23] put the solutions in the third regime, i.e. adsorption on bundled tubes. Because the nanotubes remained bundled, no PL was observed. The addition of SDBS as a highly potent dispersant individualized the tubes and lead to the ensuing PLE signal.

2.2. Excitation Transfer

PLE maps of both **C16** and SDS solubilized SWNTs (0.11 g/L) are given in **Figure 3**. A PLE map of the unbound **C16** in water is given in Figure S2 (Supporting Information). The differences between SDS (Figure 3, left) and **C16** are striking: Firstly the enhancement of the (9,5), (10,3) and (11,1) peaks in the **C16** sample can be seen at an emission wavelength of around 1260 nm. Secondly and more importantly, the **C16** solubilized sample features a massive band at excitation energies between 450 nm and 550 nm, which shows up at the emission wavelengths of all semiconducting chiralities present in the sample. This means the light is absorbed by the perylene and emitted by the tubes. Upon excitation through the perylene

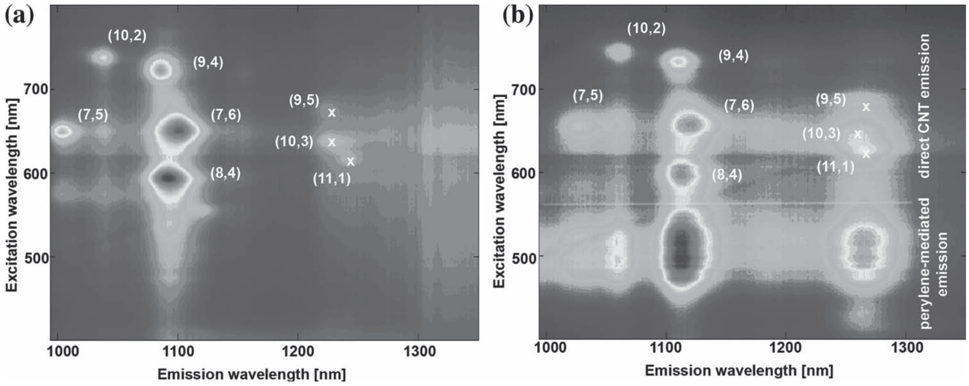

Figure 3. PLE maps of HiPCO tubes solubilized with SDS (a) and **C16** (b). The intensities are depicted linearly. A PLE map of the unbound **C16** in water is given in Figure S2 (Supporting Information).

an emission is seen at the E_{11} transition energies of all chiralities present in the sample, indicating that the process does not depend on chirality. The excitation of the perylene followed by the emission of the tubes proves a direct excitation transfer between the adsorbed perylene surfactant and the nanotubes.

The excitation transfer is highly dependent on the sample preparation conditions. PL measurements were taken at a fixed excitation wavelength of 495 nm, the peak excitation energy of perylene, for the entire batch of samples solubilized with **C16**. The samples ranged from a preparation SWNT concentration of 0.01 g/L up to 0.15 g/L. The traces thus obtained are given in **Figure 4**. Figure 4a shows the signal in the visible range, i.e., the perylene emission, while Figure 4b shows the signal trace for the samples in the infrared, i.e., the nanotube emission stemming from the indirect excitation through the adsorbed perylene surfactant. The infrared SWNT signal increases up to 0.09 g/L, then decreases again, while the perylene emission decreases with increasing nanotube preparation concentration. The SDS solubilized sample excited at 495 nm does not yield a signal.

Figure 4c–e, show three quantities extracted from the peaks around 1130 nm as seen in the IR spectra in (b). Peak intensity (Figure 4c), given here for the peak at 1130 nm, increases with nanotube preparation concentration up to 0.09 g/L and falls hereafter. The peak intensity is a good measure for the quantity of individualized and near-individualized tubes in the solution.[27–30] The process of effective solubilization and individualization is limited by the amount of surfactant available; when too much nanotube starting material is present, the surfactant fails to debundle efficiently and adsorbs to bundles instead. The surfactant covered bundles are centrifuged out, leaving behind fewer individualized nanotubes than for lower preparation concentrations. The peak position (Figure 4d) shifts towards longer wavelengths with rising nanotube concentration and ensuing falling **C16** coverage. This is attributed to the change in the dielectric

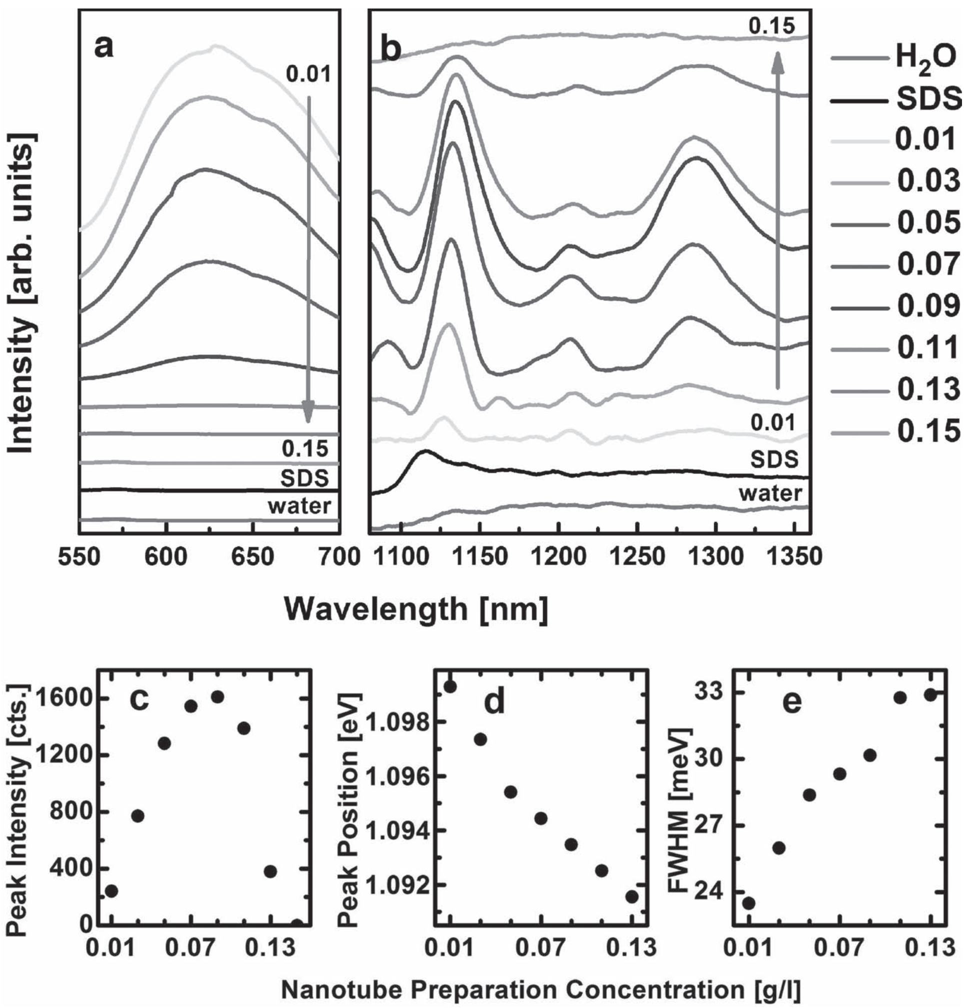

Figure 4. Photoluminescence measurements of varying preparation concentrations of SWNTs (given in g/L) solubilized with **C16**. a) Data detected with a photomultiplier. b) Data collected with an InGaAs detector. For both emission ranges the samples were excited with a fixed wavelength of 495 nm, the absorption peak of **C16**. The traces are stacked for clarity in both (a) and (b). c–e) Plots of three quantities extracted from the peaks around 1130 nm in the data displayed in (b). c) The absolute intensity of the peak around 1130 nm increases with SWNT preparation concentration up to 0.09 g/L, then decreases again. d) The peak position shifts with increasing **C16** coverage owing to the change in the dielectric environment. e) FWHM rises with nanotube preparation concentration, indicating increasing bundle size.

environment of the nanotubes.[37] Thirdly, the full width at half maximum (FWHM, Figure 4e) is a measure for debundling efficiency: narrower peaks are a sign of smaller bundles.[29] Bundle sizes increase with rising nanotube preparation concentration. At low nanotube preparation concentrations however, the concentration of free **C16** is large, as seen in Figure 4a. The second solubilization regime is characterized by a very low concentration of free perylene. We find that 0.11 g/L of nanotubes results in almost no free perylene while the concentration of individualized nanotubes is nearly optimal. The resulting degree of individualization is inferior to that for lower nanotube preparation concentrations, however, the ensuing mix of small bundles and single tubes is sufficiently individualized to be seen in PL and hence entirely satisfactory. At 0.11 g/L the **C16** emission is three orders of magnitude smaller than at 0.01 g/L, yielding a solution of individualized and near-individualized nanotubes displaying excitation transfer with hardly any free surfactant in aqueous solution.

3. Conclusions

We demonstrated that perylene-imido-diester compounds solubilize and individualize SWNTs in water as efficiently as SDS, provided the right preparation conditions are heeded. It is critical to find the right concentrations for both tubes and the perylene based surfactant, as too little surfactant results in insufficient individualization of the tubes and subsequent precipitation during centrifugation. Too much surfactant, on the other hand, leads to a surplus of free dye molecules in the solution which in turn results in a masking of the nanotube signal. The solutions prepared with **C16** are stable over the course of months.

We prove excitation transfer between the adsorbed perylene based surfactant and carbon nanotubes in the form of photoluminescence excitation measurements. The indirect excitation through the adsorbant possesses a quantum yield of the same order of magnitude as the direct excitation. This allows the collective excitation across all chiralities with a fixed wavelength in addition to individual excitation of single chiralities.

The perylene-SWNT complex subject of this study could be utilized in biomedical applications. Near-infrared spectroscopy is a well-established non-invasive method in medical diagnostics,[3,38] and the fact that nanotube-adsorbant energy transfer complexes are not confined to organic solvents any longer marks a key stepping stone towards deployment in biological environments. The enhancement in biocompatibility associated with the PG dendrons which make **C16** water soluble is well known.[26] A comprehensive study into the biocompatibility of the entire excitation-transfer complex is currently in preparation.

4. Experimental Section

The perylene compound under investigation in this study was a perylene-imido-diester with a 16-carbon double chain, referred to as **C16**:

$$\text{9,10-Bis(hexadecyloxycarbonyl)perylene-N-(methyl(1,1,1):}\ \{\text{2-oxapropyl(3, 3)}\}^{G1,G2}_{2x,4x}:\{\text{2-oxapentyl(5,4)}\}^{G3}_{8x}:\text{hydroxy}_{16}\text{-cascadane)-3,4-dicarboximide.}$$

Its chemical structure is depicted in Figure 1 (bottom panel). For the characterization see Supporting Information.

The **C16** samples were prepared at a fixed **C16** molarity of 6×10^5 M in deionized water. SWNT preparation concentrations were varied between 0.01 g/L and 0.15 g/L. Samples were tip sonicated for 90 min and subsequently centrifuged at 30 000 g and 23° for 90 min. Hereafter, only the supernatant was kept. Super purified HiPco SWNTs produced by Unidym (batch SP0295) was used for the preparation of all samples.

PLE measurements were conducted in a Horiba Nanolog system. This system featured a HgXe short arc lamp, from which a single excitation line was selected using a monochromator with two mechanically coupled gratings. The PL signals were recorded with a nitrogen-cooled InGaAs detector (infrared) and a photomultiplier (vis). The raw PLE data were fitted with Lorentzian peaks as well as both linear and constant background; the background was subsequently subtracted and the height of the Lorentzian was used as a proxy for peak intensity. All extracted data was lamp-corrected.

Absorption measurements were taken in a ThermoFisher Evolution array spectrophotometer at room temperature.

Supporting Information

Supporting Information is available from the Wiley Online Library or from the author.

Acknowledgements

F.E. and T.H. contributed equally to this work. The authors gratefully acknowledge the financial support of the European Research Commission (grant number 210642) and the German Research Foundation (DFG via SFB 658, subprojects A6 and B7) and thank Sebastian Heeg for productive discussions.

Received: March 20, 2012

---

[1] S. Reich, C. Thomsen, J. Maultzsch, *Carbon Nanotubes*, Wiley-VCH, Weinheim **2004**.

[2] A. Jorio, M. S. Dresselhaus, G. Dresselhaus, *Carbon Nanotubes - Advanced Topics in the Synthesis, Structure, Properties and Applications*, Springer, Berlin **2008**.

[3] P. Cherukuri, S. M. Bachilo, S. H. Litovsky, R. B. Weisman, *J. Am. Chem. Soc.* **2004**, *126*, 15638.

[4] N. W. S. Kam, M. O'Connell, J. A. Wisdom, H. Dai, *Proc. Natl. Acad. Sci. USA* **2005**, *102*, 11600.

[5] V. C. Moore, M. S. Strano, E. H. Haroz, R. H. Hauge, R. E. Smalley, J. Schmidt, Y. Talmon, *Nano Lett.* **2003**, *3*, 1379.

[6] V. Zorbas, A. L. Smith, H. Xie, A. Ortiz-Acevedo, A. B. Dalton, G. R. Dieckmann, R. K. Draper, R. H. Baughman, I. H. Musselman, *J. Am. Chem. Soc.* **2005**, *127*, 12323.

[7] P. W. Barone, R. S. Parker, M. S. Strano, *Anal. Chem.* **2005**, *77*, 7556.

[8] F. Lu, L. Gu, M. J. Meziani, X. Wang, P. G. Luo, L. M. Veca, L. Cao, Y.-P. Sun, *Adv. Mater.* **2009**, *21*, 139.

[9] E. Kymakis, G. A. J. Amaratunga, *Appl. Phys. Lett.* **2002**, *80*, 112.

[10] D. Baskaran, J. W. Mays, X. P. Zhang, M. S. Bratcher, *J. Am. Chem. Soc.* **2005**, *127*, 6916.

[11] A. Nish, J.-Y. Hwang, J. Doig, R. J. Nicholas, *Nanotechnology* **2008**, *19*, 095603.

[12] J. P. Casey, S. M. Bachilo, R. B. Weisman, *J. Mater. Chem.* **2008**, *18*, 1510.

[13] S. D. Stranks, J. K. Sprafke, H. L. Anderson, R. J. Nicholas, *ACS Nano* **2011**, *5*, 2307.

[14] J. K. Sprafke, S. D. Stranks, J. H. Warner, R. J. Nicholas, H. L. Anderson, *Angew. Chem. Int. Ed.* **2011**, *50*, 2313.

[15] C. Roquelet, J.-S. Lauret, V. Alain-Rizzo, C. Voisin, R. Fleurier, M. Delarue, D. Garrot, A. Loiseau, P. Roussignol, J. A. Delaire, E. Deleporte, *ChemPhysChem* **2010**, *11*, 1667.
[16] G. Magadur, J.-S. Lauret, V. Alain-Rizzo, C. Voisin, P. Roussignol, E. Deleporte, J. A. Delaire, *ChemPhysChem* **2008**, *9*, 1250.
[17] C. Backes, C. D. Schmidt, F. Hauke, C. Böttcher, A. Hirsch, *J. Am. Chem. Soc.* **2009**, *131*, 2172.
[18] C. Backes, F. Hauke, A. Hirsch, *Adv. Mater.* **2011**, *23*, 2588.
[19] C. Backes, F. Hauke, C. D. Schmidt, A. Hirsch, *Chem. Commun.* **2009**, *7345*, 2643.
[20] J. Zhao, J. P. Lu, J. Han, C.-K. Yang, *Appl. Phys. Lett.* **2003**, *82*, 3746.
[21] L. Vaisman, H. D. Wagner, G. Marom, *Adv. Colloid Interface Sci.* **2006**, *128–130*, 37.
[22] C. Ehli, C. Oelsner, D. Guldi, A. Mateo-Alonso, *Nat. Chem.* **2009**, *1*, 243.
[23] C. Backes, C. D. Schmidt, K. Rosenlehner, F. Hauke, J. N. Coleman, A. Hirsch, *Adv. Mater.* **2010**, *22*, 788.
[24] C. Backes, U. Mundloch, A. Ebel, F. Hauke, A. Hirsch, *Chem.–Eur. J.* **2010**, *16*, 3314.
[25] M. Wyszogrodzka, R. Haag, *Chem.–Eur. J.* **2008**, *14*, 9202.
[26] H. Frey, R. Haag, *Rev. Molec. Biotechnol.* **2002**, *90*, 257.
[27] S. M. Bachilo, M. S. Strano, C. Kittrell, R. H. Hauge, R. E. Smalley, R. B. Weisman, *Science* **2002**, *298*, 2361.
[28] O. N. Torrens, D. E. Milkie, M. Zheng, J. M. Kikkawa, *Nano Lett.* **2006**, *6*, 2864.
[29] P. Tan, A. Rozhin, T. Hasan, P. Hu, V. Scardaci, W. Milne, A. Ferrari, *Phys. Rev. Lett.* **2007**, *99*, 137402.
[30] C. Blum, N. Stürzl, F. Hennrich, S. Lebedkin, S. Heeg, H. Dumlich, S. Reich, M. M. Kappes, *ACS Nano* **2011**, *5*, 2847.
[31] T. Heek, C. Fasting, C. Rest, X. Zhang, F. Würthner, R. Haag, *Chem. Commun.* **2010**, *46*, 1884.
[32] W. E. Ford, *J. Photochem.* **1987**, *37*, 189.
[33] A. D. Q. Li, W. Wang, L.-Q. Wang, *Chem.–Eur. J.* **2003**, *9*, 4594.
[34] J. Kelber, H. Bock, O. Thiebaut, E. Grelet, H. Langhals, *Eur. J. Org. Chem.* **2011**, 707.
[35] L. J. Carlson, S. E. Maccagnano, M. Zheng, J. Silcox, T. D. Krauss, *Nano Lett.* **2007**, *7*, 3698.
[36] M. Jones, C. Engtrakul, W. Metzger, R. Ellingson, A. Nozik, M. Heben, G. Rumbles, *Phys. Rev. B* **2005**, *71*, 115426.
[37] J. Lefebvre, J. Fraser, Y. Homma, P. Finnie, *Appl. Phys. A: Mater. Sci. Process.* **2004**, *78*, 1107.
[38] T. K. Leeuw, R. M. Reith, R. A. Simonette, M. E. Harden, P. Cherukuri, D. A. Tsyboulski, K. M. Beckingham, R. B. Weisman, *Nano Lett.* **2007**, *7*, 2650.